JOURNAL OF AGRICULTURAL AND FOOD CHEMISTRY

pubs.acs.org/JAFC Article

Nicotinamide Alleviates Synergistic Impairment of Intestinal Barrier Caused by MC-LR and $NaNO_2$ Coexposure

Xingde Du,[#] Ruiyang Meng,[#] Houjiang Wei, Zhe Fan, Jiankang Wang, Shumeng Yuan, Kangfeng Ge, Haibin Guo, Feng Wan, Yu Fu, Fufang Wang, Xinghai Chen, Donggang Zhuang, Hongxiang Guo,* and Huizhen Zhang*

Cite This: https://doi.org/10.1021/acs.jafc.4c06756 Read Online

ACCESS | Metrics & More | Article Recommendations | Supporting Information

ABSTRACT: Microcystin-LR (MC-LR) and nitrites from the environment and daily life can be ingested and absorbed by humans via the digestive tract. However, their combined effects on intestinal health remain unclear. Here, the combined impact of MC-LR and sodium nitrite ($NaNO_2$) on the intestines of mice was investigated under actual human exposure conditions. After mice were exposed to MC-LR (10, 100 μg/L) and $NaNO_2$ (30, 300 mg/L) individual and in combination for 6 months, it was found that MC-LR and $NaNO_2$ synergistically decreased intestinal permeability and disrupted intestinal physical, chemical, immune, and microbial barriers. In the coexposure groups, the synergistic impairment to the intestinal barrier was noted with increasing concentrations of MC-LR or $NaNO_2$, but this adverse effect was alleviated by nicotinamide supplementation. This study underscores the potential risks of simultaneous ingestion of MC-LR and nitrite on intestinal health. The protective role of nicotinamide suggests avenues for therapeutic intervention against environmental toxin-induced intestinal impairment.

KEYWORDS: *microcystin-LR, nitrite, intestinal barrier, combined toxicity*

1. INTRODUCTION

Harmful algal blooms in eutrophic waters release microcystins (MCs), with microcystin-LR (MC-LR) being the most toxic and widespread variant.[1] Furthermore, nitrogen pollution in eutrophic water bodies has significantly increased due to anthropogenic nitrogen discharges and the decomposition of algae and aquatic organisms, which disrupts the nitrification process.[2] Nitrite, an intermediate product of the nitrogen cycle, can be further oxidized to nitrate. Algae absorb nitrate, which promotes their growth and results in the release of more MCs into the water.[3] This evidence highlights the severe threat that MC-LR and nitrite pose to human health and ecological security.

To protect human health from MC-LR and nitrite, the World Health Organization has set limits for MC-LR and nitrite in drinking water at 1 and 3 mg/L, respectively.[4] However, concentrations of MC-LR and nitrite in natural waters often exceed these limits by several or tens of times. For example, MC-LR levels of up to 21.7 μg/L have been detected in Bajiao Lake, China, and 236 μg/L in the Geum River Estuary, Korea.[5] In North American lakes, nitrite concentrations can reach up to 18 mg/L.[6] MC-LR and nitrite are frequently found in food products. MC-LR in leafy vegetables can reach 5.2 μg/kg[7] and 50 μg/kg in crayfish muscle tissue.[8] Nitrite levels in fruits can reach up to 2.78 mg/kg,[9] and those in processed meat products range from 7.06 to 58.77 mg/kg.[10] The tolerable daily intakes (TDIs) established by the International Agency for Research on Cancer for MC-LR [0.04 μg/kg·body weight (BW)] and nitrite (0.06 mg/kg·BW) are significantly challenged by actual daily dietary exposure to these toxicants.[11] The human health risks from long-term ingestion of MC-LR and nitrite cannot be underestimated.

The digestive tract is the main route for humans to ingest MC-LR and nitrite, with the intestines serving as the primary organ for their absorption.[12] The intestinal barrier, comprising physical, chemical, immune, and microbial components, protects against these toxicants and harmful stimuli.[13] The physical barrier includes epithelial cells and intercellular junctions,[14] the chemical barrier consists of the mucosal layer,[15] cytokines from intestinal lymphocytes maintain the immune barrier, and the microbial barrier relies on the balance of intestinal flora.[16] Disruptions to the intestinal barrier can lead to diseases such as inflammatory bowel disease (IBD),[16] acute severe pancreatitis,[17] and septicemia.[15] Epidemiological and toxicological studies suggest that MC-LR and nitrite exposure individually have toxic effects on intestinal health and may be linked to IBD and colorectal cancer.[18,19] However, the combined effects of MC-LR and nitrite on the mammalian intestines remain unexplored.

Niacinamide (NAM), a form of vitamin B3, is extensively used in foods and beverages to enhance nutritional value, prevent niacin deficiency, and improve metabolic function and skin health.[20] Its antioxidant properties extend shelf life and

Received: July 26, 2024
Revised: October 2, 2024
Accepted: October 3, 2024

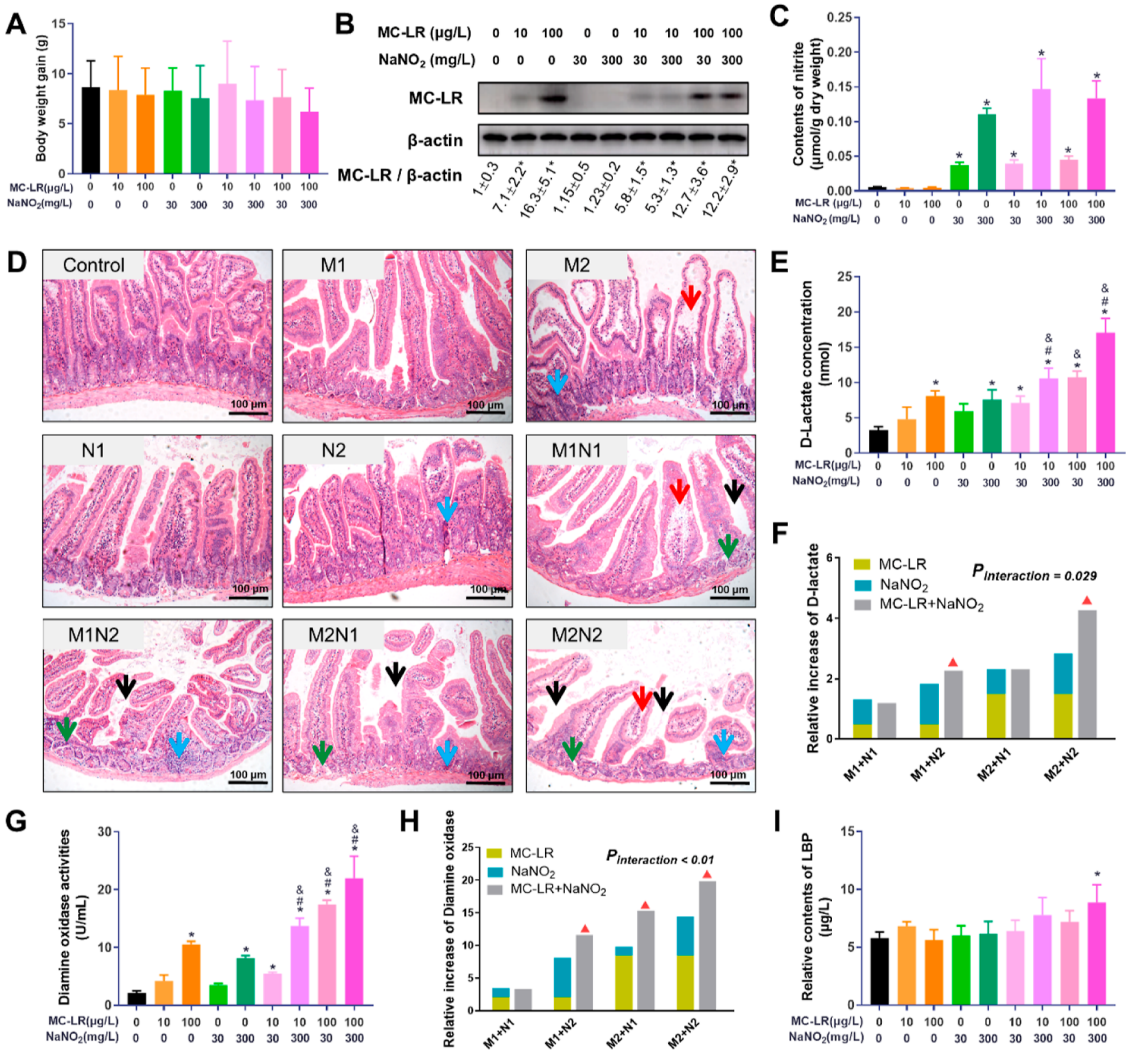

Figure 1. Effects of MC-LR and $NaNO_2$ combined exposure on the intestines in mice. (A) Changes in the body weight of mice were analyzed. (B) Relative contents of MC-LR in the intestinal tissues were analyzed by Western Blot. (C) Concentrations of $NaNO_2$ in mouse intestinal tissues were detected by the Elisa kit. (D) Histopathological changes in the intestinal tissue of mice were observed by H&E staining. Red arrows: intestinal epithelial cell loss and intestinal villi lysis; blue arrows: inflammatory cell infiltration; black arrows: sparsely arranged, reduced number and shorter length of intestinal villi; green arrows: structural disorganization of intestinal mucosa, glandular atrophy. Concentrations of D-lactate (E) and diamine oxidase (G) in mouse serum were detected by Elisa kit, and the combined effects of MC-LR and $NaNO_2$ on D-lactate (F) and diamine oxidase (H) were analyzed. (I) The content of serum LBP in mice was detected by the Elisa kit. ▲ indicates a synergistic toxic effect of MC-LR and $NaNO_2$ coexposure. *$P < 0.05$, versus the control group; #$P < 0.05$, versus corresponding MC-LR group; &$P < 0.05$, versus corresponding $NaNO_2$ group.

enhance stability during food processing. Consequently, NAM is crucial for enhancing food quality, nutrition, and health benefits. Recently, NAM has been used as a pharmaceutical and nutritional supplement because of its neuroprotective, anti-inflammatory, and antifibrotic properties.[21] Numerous studies have linked NAM metabolism to intestinal homeostasis and alleviation of IBD. "Nicotinate and nicotinamide metabolism" is a major metabolic feature in inflamed tissues of ulcerative colitis.[22] Increasing NAM levels may enhance the protective function of the intestinal barrier and could be considered a therapeutic approach for IBD intervention.[23] Nevertheless, the protective role of niacinamide against damage to the intestines caused by environmental toxicants remains unclear.

Thus, our goal was to investigate the impact of chronic exposure to nitrite and MC-LR on the intestines of mice and to identify potential intervention strategies. Specifically, we examined the individual and combined effects of nitrite and MC-LR, at concentrations relevant to human exposure, on intestinal functions and barriers in mice. Additionally, we explored how NAM regulates intestinal damage resulting from coexposure to MC-LR and nitrite based on the results from 16S rRNA sequencing. This study provides valuable insights and therapeutic approaches to address intestinal impairment caused by the combined exposure to MC-LR and nitrite.

2. MATERIALS AND METHODS

2.1. Regents. Details information is provided in the Supporting Information 1.1.

2.2. Animal Treatment. Details information is provided in the Supporting Information 1.2.

2.3. Cell Experiments. Details information is provided in the Supporting Information 1.3.

2.4. Hematoxylin and Eosin (H&E) Staining. Details information is provided in the Supporting Information 1.4.

https://doi.org/10.1021/acs.jafc.4c06756
J. Agric. Food Chem. XXXX, XXX, XXX−XXX

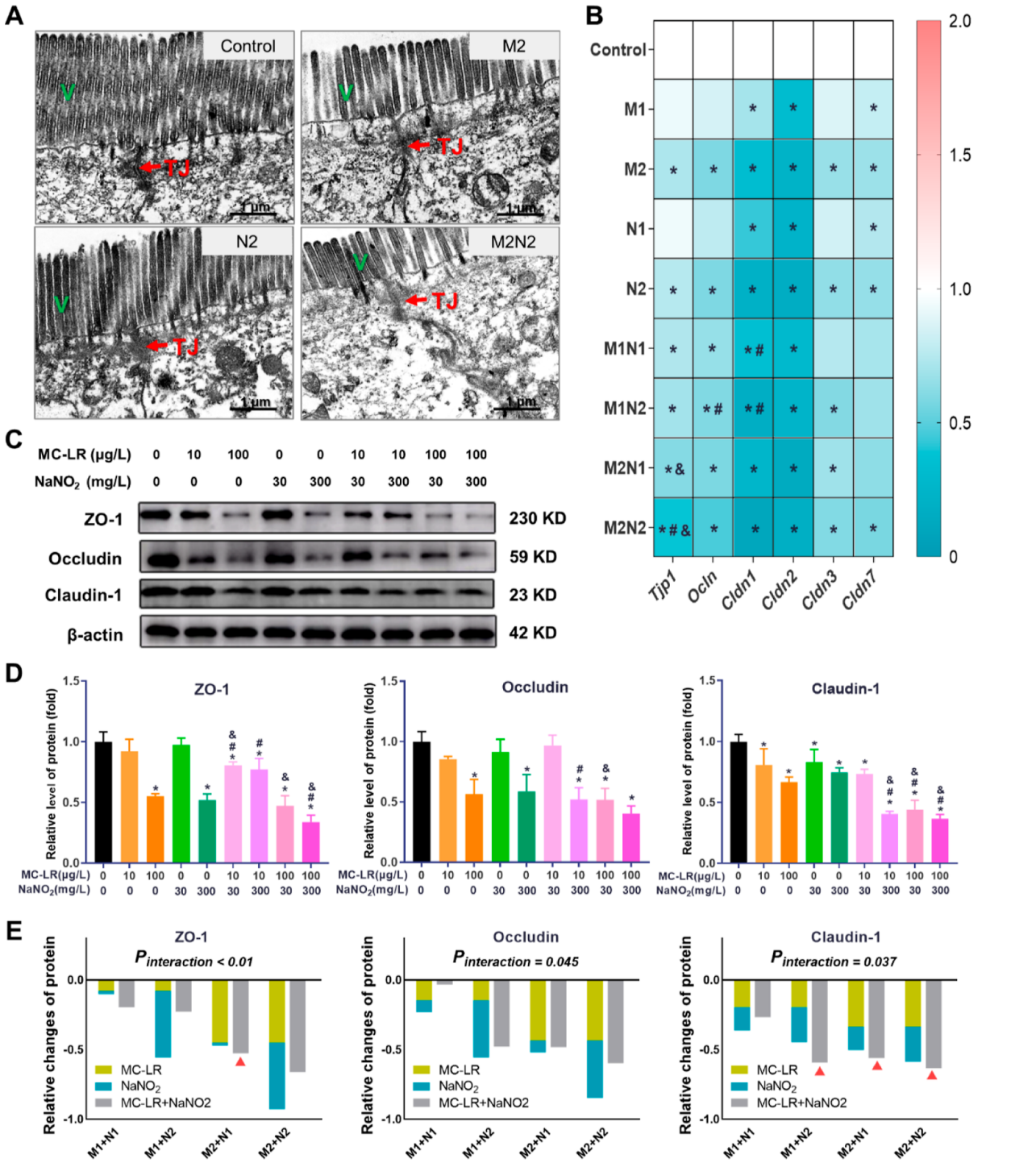

Figure 2. Effects of combined exposure of MC-LR and $NaNO_2$ on the physical barrier of intestines in mice. (A) Ultrastructural alterations of the intestines were observed by electron microscopy (V: microvilli; TJ: tight junction). (B) The mRNA expressions of the tight junction-related genes *Tjp1*, *Ocln*, *Cldn1*, *Cldn2*, *Cldn3*, and *Cldn7* in mouse intestinal tissues were detected by qPCR. (C,D) The protein levels of tight junction-related proteins ZO-1, Occludin, and Claudin-1 in mouse intestinal tissues were detected by Western Blot and quantified using ImageJ. (E) The combined effects of MC-LR and $NaNO_2$ on ZO-1, Occludin, and Claudin-1 levels were analyzed. ▲ indicates a synergistic toxic effect of MC-LR and $NaNO_2$ coexposure. $^{*}P < 0.05$, versus the control group; $^{\#}P < 0.05$, versus corresponding MC-LR group; $^{\&}P < 0.05$, versus corresponding $NaNO_2$ group.

2.5. Assay of $NaNO_2$ Concentration in Intestinal Tissues. Details information is provided in the Supporting Information 1.5.

2.6. Western Blot and Dot Blot. Details information is provided in the Supporting Information 1.6.

2.7. Determination of Serum D-Lactic Acid, Diamine Oxidase, and Lipopolysaccharide Binding Protein. Details information is provided in the Supporting Information 1.7.

2.8. Determination of NAM. Details information is provided in the Supporting Information 1.8.

2.9. Transmission Electron Microscope. Details information is provided in the Supporting Information 1.9.

2.10. Real-Time Quantitative Polymerase Chain Reaction (qPCR). Details information is provided in the Supporting Information 1.10.

https://doi.org/10.1021/acs.jafc.4c06756
J. Agric. Food Chem. XXXX, XXX, XXX−XXX

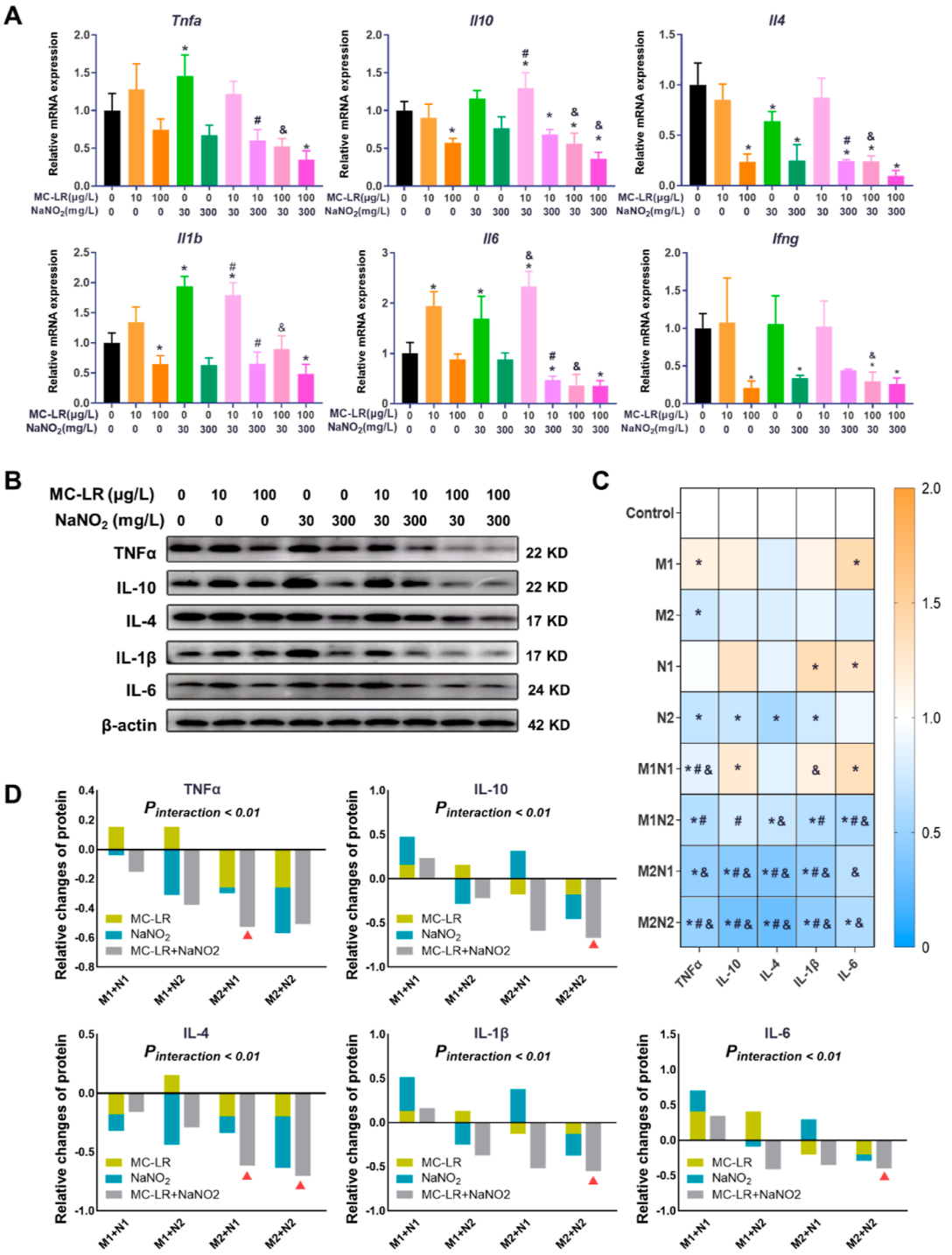

Figure 3. Effects of coexposure of MC-LR and $NaNO_2$ on the immune barrier of intestines in mice. (A) The mRNA expressions of inflammation-related genes *Tnfa*, *Il10*, *Il4*, *Il1b*, *Il6*, and *Ifng* in mouse intestinal tissues were detected by qPCR. (B,C) Protein levels of inflammation-related factors TNFα, IL-10, IL-4, IL-1β, and IL-6 in mouse intestinal tissues were measured by Western Blot and quantified by ImageJ. (D) The combined effects of MC-LR and $NaNO_2$ on TNFα, IL-10, IL-4, IL-1β, and IL-6 levels were analyzed. ▲ indicates a synergistic toxic effect of MC-LR and $NaNO_2$ coexposure. $^{*}P < 0.05$, versus the control group; $^{\#}P < 0.05$, versus corresponding MC-LR group; $^{\&}P < 0.05$, versus corresponding $NaNO_2$ group.

2.11. Periodic Acid-Schiff Staining (PAS Staining). Details information is provided in the Supporting Information 1.11.

2.12. Immunohistochemical Staining. Details information is provided in the Supporting Information 1.12.

2.13. 16S RNA Sequencing. Details information is provided in the Supporting Information 1.13.

2.14. Statistical Analysis. Details information is provided in the Supporting Information 1.14.

3. RESULTS

3.1. Impact of Combined MC-LR and $NaNO_2$ Exposure on the Intestines of Mice. After six months of exposure to different concentrations of MC-LR (10, 100 μg/L) and $NaNO_2$ (30, 300 mg/L), mice showed no significant changes in body weight (Figure 1A). The concentrations of MC-LR and $NaNO_2$ in the intestinal tissues increased in a dose-

https://doi.org/10.1021/acs.jafc.4c06756
J. Agric. Food Chem. XXXX, XXX, XXX−XXX

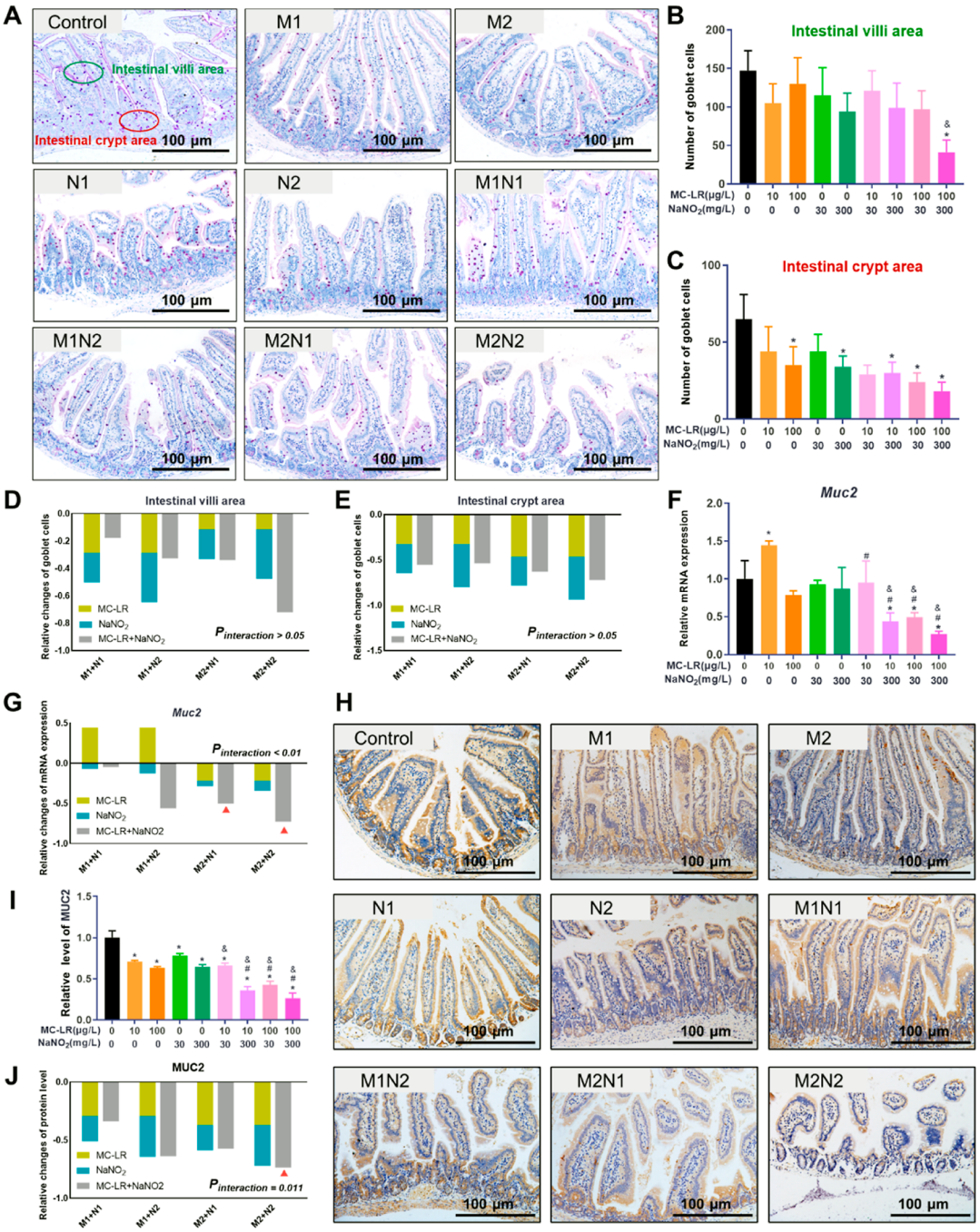

Figure 4. Changes in the chemical barrier of the intestines of mice after the combined exposure to MC-LR and $NaNO_2$. (A) Goblet cells in intestinal tissue were observed by PAS staining, and the number of goblet cells in intestinal villi (green circle) and crypts area (red circle) was analyzed, respectively (B,C). (D,E) The combined effects of MC-LR and $NaNO_2$ on the changes in goblet cells were analyzed. (F) The mRNA expression of *Muc2* in mouse intestinal tissues was detected by qPCR. (G) The combined effect of MC-LR and $NaNO_2$ on *Muc2* expression was analyzed. (H,I) The MUC2 protein level in mouse intestinal tissues was observed by immunohistochemical staining and quantified using ImageJ. (J) The combined effects of MC-LR and $NaNO_2$ on the changes in MUC2 level were analyzed. ▲ indicates a synergistic toxic effect of MC-LR and $NaNO_2$ coexposure. $^{*}P < 0.05$, versus the control group; $^{\#}P < 0.05$, versus corresponding MC-LR group; $^{\&}P < 0.05$, versus corresponding $NaNO_2$ group.

dependent manner with higher exposure levels. However, no significant changes in MC-LR or $NaNO_2$ levels after their coexposure were observed compared to the individual exposure group. This suggests that $NaNO_2$ exposure did not affect the accumulation of MC-LR in the intestines of mice (Figure 1B,C). In Control, M1 (10 μg/L MC-LR), and N1 (30 mg/L $NaNO_2$) groups, intestinal structure appeared normal with neatly arranged epithelial cells and intact villi. However, higher concentrations (M2: 100 μg/L MC-LR, N2: 300 mg/L $NaNO_2$) caused minor pathological changes, including inflammation and villi damage. Combined exposure of MC-LR and $NaNO_2$ resulted in severe intestinal injuries, such as villi shortening, epithelial cell loss, and mucosal disorganization (Figure 1D). D-Lactate levels and diamine oxidase activities, indicators of intestinal barrier function, significantly increased in mouse serum after exposure to 100 μg/L MC-LR and 300

https://doi.org/10.1021/acs.jafc.4c06756
J. Agric. Food Chem. XXXX, XXX, XXX−XXX

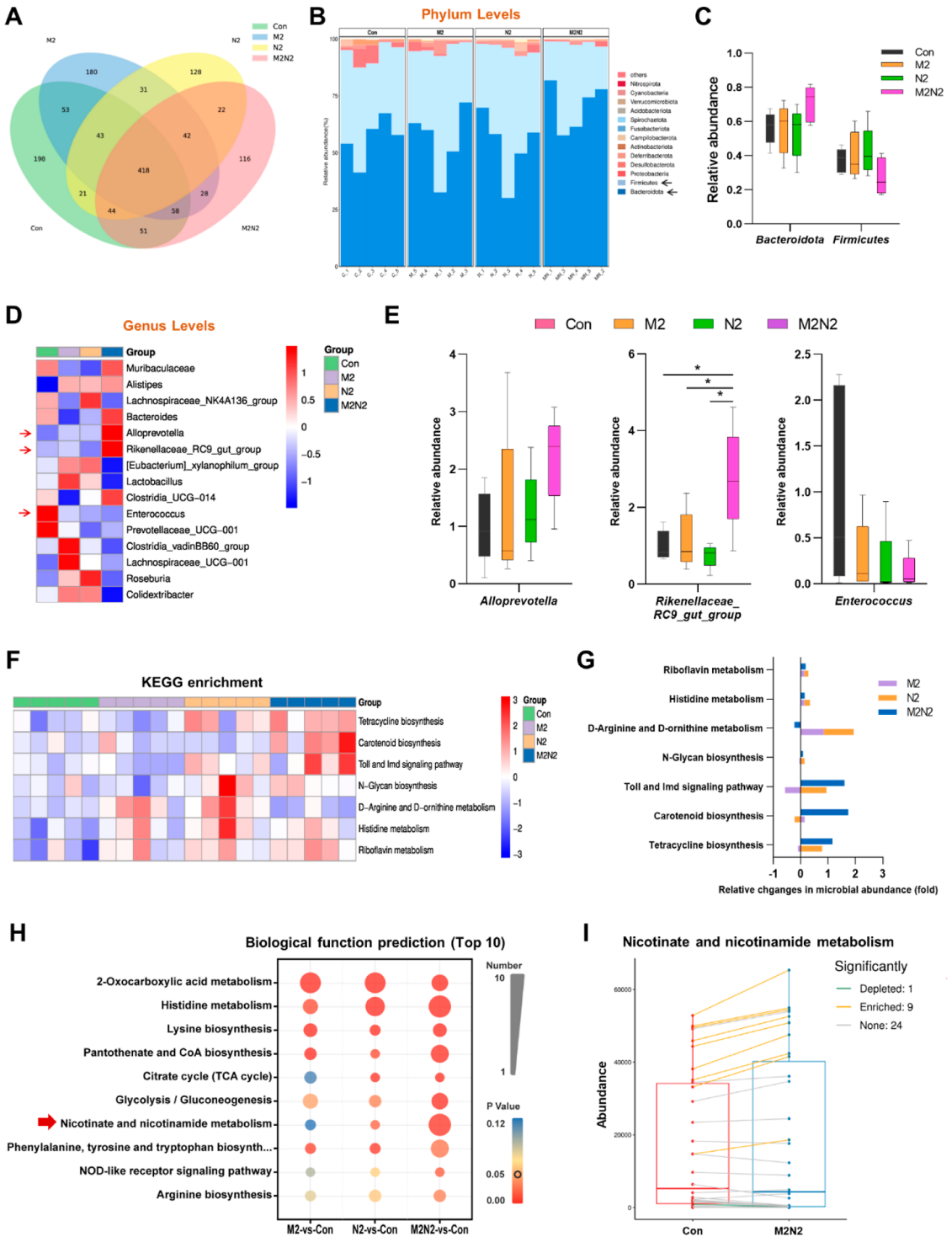

Figure 5. Alterations of the microbial barrier in the intestines of mice after MC-LR and $NaNO_2$ coexposure. (A) The shared and unique microbial information across all groups was shown in the Venn diagram. (B) Changes in microbial composition at the phylum level among different groups were presented. (C) Relative abundances of *Bacteroidota* and *Firmicutes* at the phylum level were analyzed. (D) Alterations in microbial composition at the genus level from different groups were analyzed, and the relative abundance of genera with potential synergistic effects (red arrows) after coexposure to MC-LR and $NaNO_2$ were presented. (E) The combined effect of MC-LR and $NaNO_2$ on the changes of the genus *Rikenellaceae RC9_gut_group* was analyzed. (F–I) Predicted functions of intestinal microbes in mice based on the Kyoto Encyclopedia of Genes and Genomes (KEGG) and COG databases. *$P < 0.05$.

mg/L $NaNO_2$ individual and in combination ($P < 0.05$) (Figure 1E,F). Synergistic impairments of MC-LR and $NaNO_2$ on these indicators were observed (Figure 1G,H). Elevated serum lipopolysaccharide binding protein (LBP) levels further indicated compromised intestinal barrier integrity (Figure 1I).

3.2. Physical Barrier Disruption in the Intestines of Mice by MC-LR and $NaNO_2$ Coexposure. The intestinal physical barrier, crucial for maintaining integrity, primarily comprises intercellular tight junctions.[24] In the control group, intestinal epithelial microvilli were abundant and well-organ-

https://doi.org/10.1021/acs.jafc.4c06756
J. Agric. Food Chem. XXXX, XXX, XXX−XXX

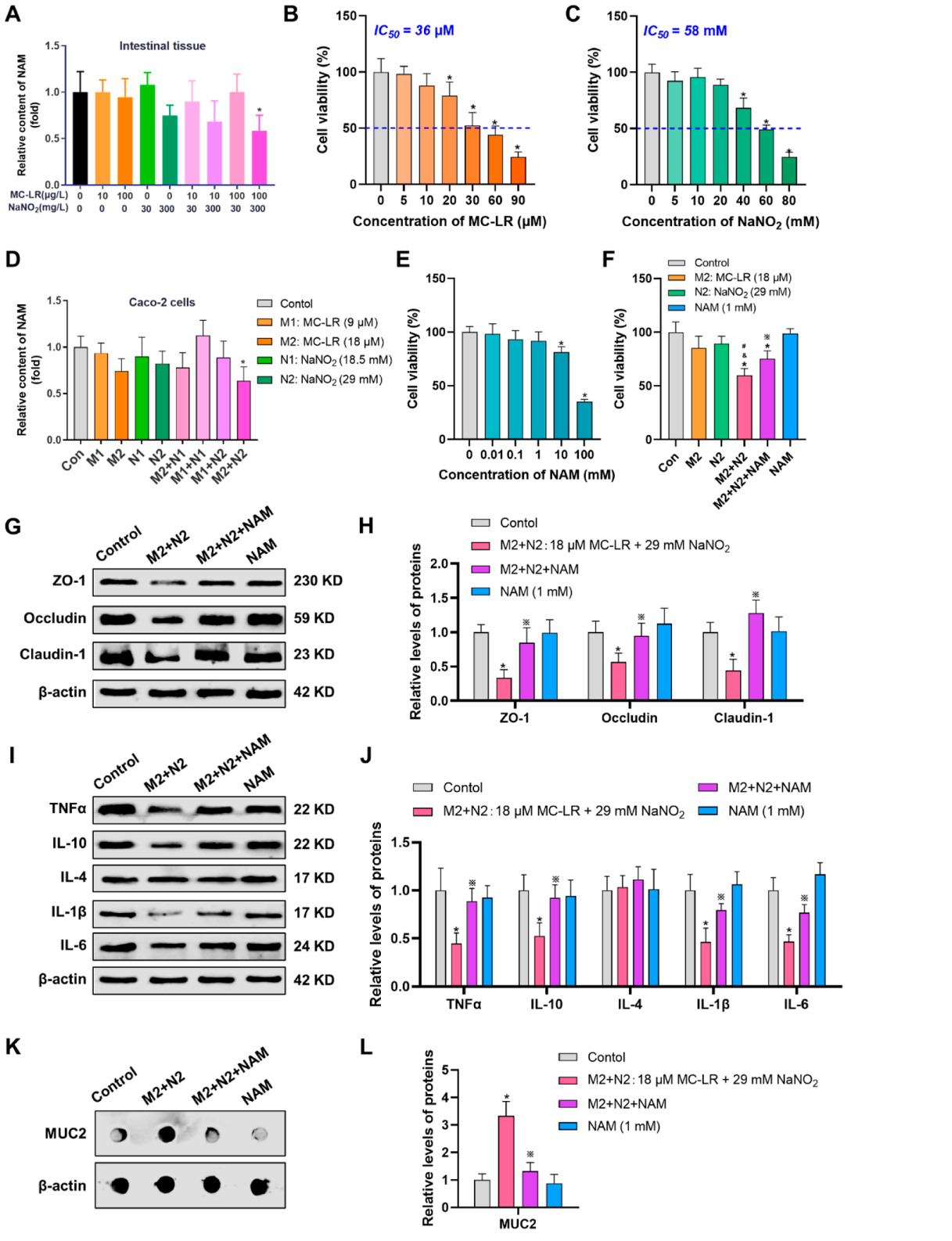

Figure 6. Effects of NAM supplementation on MC-LR and $NaNO_2$ coexposure-induced intestinal function impairment. (A) NAM levels in mouse intestinal tissues were detected by ELISA kit. (B,C) The effect of MC-LR and $NANO_2$ on Caco-2 cell viability was analyzed by the CCK8 kit. (D) NAM levels in Caco-2 cells were detected by ELISA kit. (E,F) Effects of NAM, MC-LR, and $NaNO_2$ exposure alone and in combination on Caco-2 cell viability were analyzed using the CCK8 kit. (G–J) Tight junction-associated proteins (ZO-1, Occludin, and Claudin-1) and inflammation-associated proteins (TNFα, IL-10, IL-4, IL-1β, IL-6) were detected by Western Blot and quantified by ImageJ. (K,L) The level of the mucin MUC2 was detected by Dot Blot and quantified by ImageJ. $^{*}P < 0.05$, versus the control group; $^{\#}P < 0.05$, versus corresponding MC-LR group; $^{\&}P < 0.05$, versus corresponding $NaNO_2$ group. $^{※}P < 0.05$, versus the MC-LR + $NaNO_2$ group.

https://doi.org/10.1021/acs.jafc.4c06756
J. Agric. Food Chem. XXXX, XXX, XXX−XXX

ized, and tight junctions remained intact. In the M2 and N2 groups, the tight junctions between intestinal epithelial cells were sparsely structured, the microvilli on the surface of the intestinal epithelial cells were shortened, and the tight junctions were diffuse or even broken. In the M2N2 group, the tight junction structure was disrupted more severely, suggesting that the tight junctions were more severely disrupted by MC-LR and $NaNO_2$ coexposure (Figure 2A). This disruption is corroborated by assays of tight junction-related genes (Figure 2B) and proteins (Figure 2C). Compared to MC-LR or $NaNO_2$ individual, their combined exposure significantly down-regulates the levels of Zonula occludens-1 (ZO-1) and Claudin-1 ($P < 0.05$) (Figure 2D). Co-exposure of MC-LR with $NaNO_2$ at specific concentrations showed a synergistic effect on altering ZO-1 and Claudin-1 protein levels (Figure 2E).

3.3. Immune Barrier Dysfunction in the Intestines of Mice Caused by MC-LR and $NaNO_2$ Combined Exposure. Homeostasis of the intestinal immune system is crucial for maintaining intestinal function. In mice exposed to different concentrations of MC-LR and $NaNO_2$, distinct patterns of inflammatory factor expression were observed. As shown in Figure 3A, mice exposed to 10 μg/L MC-LR and 30 mg/L $NaNO_2$ showed increased expression levels of the inflammatory factors *Tnfa*, *Il6*, and *Il1b*. Conversely, exposure to 100 μg/L MC-LR and 300 mg/L $NaNO_2$ decreased expressions of *Tnfa*, *Il10*, *Il4*, *Il1b*, and *Ifng*. Combined exposure to 100 μg/L MC-LR and 300 mg/L $NaNO_2$ significantly decreased the levels of *Tnfa*, *Il10*, *Il4*, *Il1b*, *Il6*, and *Ifng* in mouse intestinal tissues ($P < 0.05$). Corresponding protein levels demonstrated significant decreases in TNFα, IL-10, IL-4, and IL-1β compared to Control, MC-LR, or $NaNO_2$ groups after coexposure ($P < 0.05$) (Figure 3B,C). Synergistic effects of MC-LR (100 μg/L) and $NaNO_2$ (300 mg/L) on inflammation-related factors IL10, IL4, IL-1β, and IL-6 were evident in protein level alterations (Figure 3D).

3.4. Chemical Barrier Disorder in the Intestines of Mice Following MC-LR and $NaNO_2$ Coexposure. Mucin 2 (MUC2), which is secreted by goblet cells, plays a critical role in maintaining the intestinal chemical barrier. Combined exposure to MC-LR and $NaNO_2$ leads to a significant decrease in goblet cells within the intestinal villi and crypts ($P < 0.05$) (Figure 4A−C). However, there were no significant synergistic effects on the reduction of intestinal villi (Figure 4D,E). Further investigation showed that the levels of mRNA (Figure 4F,G) and protein (Figure 4H,J) of MUC2 were significantly down-regulated after the combined exposure of MC-LR and $NaNO_2$ ($P < 0.05$).

3.5. Microbial Barrier Disturbance in the Intestines of Mice after MC-LR and $NaNO_2$ Combined Exposure. Chronic exposure of mice to MC-LR (100 μg/L) and $NaNO_2$ (300 mg/L) resulted in significant synergistic damage to the physical, immune, and chemical barriers of the intestines. To further understand the effects of MC-LR and $NaNO_2$ on the intestinal microbes and their roles in intestinal barriers, mouse feces from the Control, M2, N2, and M2N2 groups were analyzed by 16sRNA sequencing. There are 418 shared microbial types among all groups, with unique species in Control (198), M2 (180), N2 (128), and M2N2 (116) (Figure 5A). *Bacteroidota* and *Firmicutes* predominated at the phylum level (Figure 5B), with a shift toward increased *Bacteroidota* and decreased *Firmicutes* after MC-LR and $NaNO_2$ exposure (Figure 5C). At the genus levels, the genera *Alloprevotella*, *Rikenellaceae RC9_gut_group*, and *Enterococcus* were altered after combined exposure to MC-LR and $NaNO_2$ (Figure 5D,E). The functional analysis highlighted changes in biological processes, including tetracycline biosynthesis, carotenoid biosynthesis, and toll and imd signaling pathway (Figure 5F), albeit without synergistic effect (Figure 5G). The Cluster of Orthologous Groups of proteins (COG)-based predictions indicated significant enrichment in "Nicotinate and nicotinamide metabolism" following combined exposure to MC-LR and $NaNO_2$ compared to individual exposure (Figure 5H), with nine associated microbial types showing increased abundance (Figure 5I).

3.6. NAM Supplementation Mitigates Intestinal Impairment Induced by MC-LR and $NaNO_2$ Coexposure. The NAM level in mouse intestinal tissues showed a significant decrease after combined exposure to MC-LR and $NaNO_2$ was observed (Figure 6A). Therefore, the role of NAM in mitigating intestinal function disruption caused by MC-LR and $NaNO_2$ coexposure was further investigated in vitro. The half-maximal inhibitory concentration (IC_{50}) of MC-LR and $NaNO_2$ for Caco-2 cells were 36 and 58 mM, respectively (Figure 6B,C). The 1/2 IC_{50} of MC-LR (18 μM) and $NaNO_2$ (29 mM) were used as the exposure concentration in cell experiments. Exposure to MC-LR and $NaNO_2$ resulted in decreased NAM levels in Caco-2 cells. The no-observed-adverse-effect-level (NOAEL) of NAM on Caco-2 cells was 1 mM (Figure 6E), which was used for in vitro intervention. NAM supplementation significantly alleviated the decrease in cell viability induced by combined exposure to MC-LR and $NaNO_2$ ($P < 0.05$) (Figure 6F). Further investigations showed that NAM supplementation mitigated the reduction in tight junction proteins (ZO-1, Occludin, and Claudin-1) induced by MC-LR with $NaNO_2$ in Caco-2 cells ($P < 0.05$) (Figure 6G,H). Additionally, NAM attenuated the decrease in immune-related proteins (TNFα, IL-10, IL-1β, and IL-6) (Figure 6I,J) and mucin MUC2 (Figure 6K,L), caused by MC-LR and $NaNO_2$ coexposure ($P < 0.05$).

4. DISCUSSION

This study represents the first investigation into the adverse effects resulting from combined exposure to MC-LR and $NaNO_2$ on intestinal barrier function, emphasizing its significance in understanding potential disease development.[25,26] Notably, MC-LR and nitrite were detected in mouse intestinal tissues following six months of MC-LR and $NaNO_2$ exposure. This indicates that MC-LR and $NaNO_2$ are capable of accumulating in small intestinal tissues, serving as a prerequisite for the two toxicants to induce intestinal toxicity.

The intestine plays a crucial role in the digestion and absorption of nutrients while also acting as a barrier to prevent the invasion of toxicants.[27] Previous studies have demonstrated that MC-LR in the gastrointestinal tract can damage the structure of the intestinal villus.[28] Acute exposure to $NaNO_2$ caused significant histomorphology changes in the intestines of rats, resulting in swelling and structural damage of villi.[29] This study observed histopathological alterations in the intestines following long-term exposure to MC-LR and $NaNO_2$. In contrast, coexposure of MC-LR and $NaNO_2$ resulted in more severe damaging effects, which can be confirmed by the results of the intestinal barrier evaluation indicators such as D-lactate[30] and diamine oxidase.[31] The impaired intestinal barrier allows toxic metabolite lipopolysaccharide (LPS) from intestinal bacteria to enter the bloodstream, potentially leading to

https://doi.org/10.1021/acs.jafc.4c06756
J. Agric. Food Chem. XXXX, XXX, XXX−XXX

infections and diseases such as immune imbalance, IBD, and malnutrition.[32] Increased serum LBP levels and disturbed intestinal immunity observed in our study further support this understanding. Following this, the systemic effects of MC-LR and $NaNO_2$ on the intestines were elaborated from the perspectives of the physical, chemical, immune, and microbial barriers.

The tight junction proteins Occludin, Claudins, and ZO-1 are vital for maintaining the intestinal physical barrier.[33] The cytoplasmic scaffold protein ZO-1 can bind Claudins to the actin cytoskeleton, ensuring tight junction integrity, while Occludin interacts with Claudins to stabilize tight junctions and regulate cell permeability.[33,34] Dysfunction of these tight junctions can lead to increased intestinal permeability, a significant concern in IBD.[35] Our study revealed that combined exposure to MC-LR and $NaNO_2$ down-regulated Claudin-1, ZO-1, and Occludin levels in mouse intestinal tissues, disrupting tight junction ultrastructure, compromising the physical barrier.

The intestines also serve as a major immune organ, where the immune barrier plays a crucial role in responding to pathogens.[36] Intestinal epithelial and immune cells initiate inflammatory responses upon detecting pathogens, releasing pro-inflammatory cytokines like IL-1, IL-6, and TNF-α, which are essential for managing inflammation.[37] Our findings showed that exposure to MC-LR and $NaNO_2$ increased levels of TNF-α, IL-1β, and IL-6 while decreasing IL-4, indicating an inflammatory response. However, MC-LR and $NaNO_2$ coexposure resulted in significant suppression of inflammatory factors, suggesting severe damage to the intestinal immune system and potential immunosuppression.[38]

MUC2, secreted by goblet cells, forms a protective mucosal barrier in the gastrointestinal epithelium.[39] The mucosal chemical barrier of the intestines provides further protection against mechanical stress, harmful substances, bacteria, and pathogens, thereby preventing intestinal-associated diseases.[40] MUC2 deficiency can lead to colitis, highlighting its essential role in defending against intestinal diseases.[41] Our study found that combined exposure to MC-LR and $NaNO_2$ significantly reduced goblet cell numbers and MUC2 levels, compromising the intestinal chemical barrier.

Intestinal microbes play a crucial role in preserving barrier integrity and immune regulation.[42] Our findings indicate that simultaneous exposure to MC-LR and $NaNO_2$ significantly reduced microbial diversity and altered the abundance of specific genera, such as *Alloprevotella* and *Rikenellaceae RC9_gut_group*, which are linked to increased susceptibility to intestinal diseases.[43,44] The reduction of the abundance of beneficial *Enterococcus* further exacerbates the risk of infections and inflammatory responses in the intestines.[45] Additionally, the prediction of the biological functions among the altered intestinal microbes revealed significant enrichment in the nicotinate and NAM metabolism pathway following coexposure to MC-LR and $NaNO_2$, a change not observed with either toxin individually, raising our concern.

While the combined toxicity of MC-LR and $NaNO_2$ exhibits universality in some aspects, the mechanism of their synergistic effects may differ among organs. For instance, $NaNO_2$ exacerbates MC-LR-induced spleen damage and innate immune dysfunction in zebrafish through oxidative stress.[46] Combined exposure to MC-LR and $NaNO_2$ has been found to induce synergistic reproductive toxicity via the HPG axis[47] and mitochondrial dysfunction.[48] Moreover, MC-LR and $NaNO_2$ coexposure can disrupt hepatic lipid metabolism through the NRF2/HO-1 pathway.[49] Our evidence from 16S rRNA sequencing and in vitro experiments suggests that MC-LR and $NaNO_2$ can lead to indirect toxic effects on the intestines by interfering with the same biological signaling pathway (NAM metabolism), implying that NAM metabolism disruption could be a key mechanism of intestinal injury caused by their combined exposure.

Abnormalities in nicotinamide metabolism are characteristic of intestinal disease.[22] In particular, NAM has been shown to protect the intestinal barrier from chemical toxins.[50] Previous studies have shown that NAM mitigates ethanol-induced tight junction damage by modulating mitochondrial function,[51] a process influenced by oxidative stress resulting from mitochondrial dysfunction.[52] Mitochondrial dysfunction and oxidative stress can lead to apoptosis, reducing goblet cell numbers and MUC2 secretion.[53] Given its potential antioxidant properties, NAM may alleviate tight junction damage and mucin secretion deficits resulting from combined MC-LR and $NaNO_2$ exposure, safeguarding both physical and chemical barriers.

Moreover, the anti-inflammatory properties of NAM have been well corroborated. In diabetic rat models, NAM intervention significantly reduced abnormal inflammatory cytokines levels such as IL-6 and TNFα.[54] Another study indicated that NAM can alleviate dextran sulfate sodium-induced colitis in C57BL/6 mice by regulating metabolic homeostasis of short-chain fatty acids and inflammatory cytokine production.[55] Our study presents the first evidence that NAM supplementation can alleviate the damage to intestinal physical, chemical, and immune barriers induced by MC-LR and $NaNO_2$ coexposure in vitro. However, further confirmation through in vivo models, including flora transplantation and NAM supplementation, is warranted.

In conclusion, MC-LR and $NaNO_2$ can accumulate in the intestines of mice, damaging the structure and function of intestinal tissues, increasing permeability, and disrupting the intestinal barrier, resulting in synergistic toxicity. Specifically, their combined exposure destroys intestinal tight junctions, dysregulates the immune system, reduces MUC2 levels, and disrupts microbial homeostasis, impairing intestinal barriers. NAM supplementation can mitigate these adverse effects induced by MC-LR and $NaNO_2$. These findings shed light on the etiology of intestinal diseases linked to environmental factors and suggest that NAM could serve as a potential therapy to alleviate intestinal damage from pollutants. We emphasize the benefits of NAM supplementation and recommend it as a proactive measure to prevent and protect the health of individuals at risk for intestinal diseases.

■ ASSOCIATED CONTENT

Supporting Information

The Supporting Information is available free of charge at https://pubs.acs.org/doi/10.1021/acs.jafc.4c06756.

Detailed information on materials and methods used in this study, including regents, animal treatment, cell experiments, H&E staining, assays for $NaNO_2$ concentration in intestinal tissues, Western blot and dot blot analyses, determination of serum D-lactic acid, diamine oxidase, and LBP, determination of NAM, transmission electron microscopy, qPCR, PAS staining, immunohistochemical staining, 16S RNA sequencing, and statistical

https://doi.org/10.1021/acs.jafc.4c06756
J. Agric. Food Chem. XXXX, XXX, XXX−XXX

analysis. The primer sequences used in qPCR can be found in Table S1 (PDF)

AUTHOR INFORMATION

Corresponding Authors

Hongxiang Guo − *College of Life Sciences, Henan Agricultural University, Zhengzhou, Henan 450002, China*; Email: guohongxiang06@126.com

Huizhen Zhang − *College of Public Health, Zhengzhou University, Zhengzhou, Henan 450001, China*; orcid.org/0000-0002-0255-1856; Email: huizhen18@126.com

Authors

Xingde Du − *College of Public Health, Zhengzhou University, Zhengzhou, Henan 450001, China*

Ruiyang Meng − *College of Public Health, Zhengzhou University, Zhengzhou, Henan 450001, China*

Houjiang Wei − *School of Henan Medical, Zhengzhou University, Zhengzhou, Henan 450001, China*

Zhe Fan − *School of Henan Medical, Zhengzhou University, Zhengzhou, Henan 450001, China*

Jiankang Wang − *School of Henan Medical, Zhengzhou University, Zhengzhou, Henan 450001, China*

Shumeng Yuan − *College of Public Health, Zhengzhou University, Zhengzhou, Henan 450001, China*

Kangfeng Ge − *College of Public Health, Zhengzhou University, Zhengzhou, Henan 450001, China*

Haibin Guo − *The Reproductive Medicine Center, Henan Provincial People's Hospital, Zhengzhou, Henan 450003, China*

Feng Wan − *The Reproductive Medicine Center, Henan Provincial People's Hospital, Zhengzhou, Henan 450003, China*

Yu Fu − *College of Public Health, Zhengzhou University, Zhengzhou, Henan 450001, China*

Fufang Wang − *College of Public Health, Zhengzhou University, Zhengzhou, Henan 450001, China*

Xinghai Chen − *Department of Chemistry and Biochemistry, St Mary's University, San Antonio, Texas 78228, United States*

Donggang Zhuang − *College of Public Health, Zhengzhou University, Zhengzhou, Henan 450001, China*

Complete contact information is available at: https://pubs.acs.org/10.1021/acs.jafc.4c06756

Author Contributions

#X.D. and R.M. contributed equally to this work.

Funding

This work was supported by the National Natural Science Foundation of China (nos 82073512, 82273594) and the Leading Talents in Science and Technology Innovation Program of Zhongyuan (no. 244200510028).

Notes

The authors declare no competing financial interest.

REFERENCES

(1) Zeng, Y. H.; Cai, Z. H.; Zhu, J. M.; Du, X. P.; Zhou, J. Two hierarchical LuxR-LuxI type quorum sensing systems in Novosphingobium activate microcystin degradation through transcriptional regulation of the mlr pathway. *Water Res.* **2020**, *183*, 116092.

(2) Zhu, L.; Shi, W.; Van Dam, B.; Kong, L.; Yu, J.; Qin, B. Algal Accumulation Decreases Sediment Nitrogen Removal by Uncoupling Nitrification-Denitrification in Shallow Eutrophic Lakes. *Environ. Sci. Technol.* **2020**, *54* (10), 6194−6201.

(3) Kieley, C. M.; Roelke, D. L.; Park, R.; Campbell, K. L.; Klobusnik, N. H.; Walker, J. R.; Cagle, S. E.; Kneer, M. L.; Stroski, K. M.; Brooks, B. W.; et al. Concentration of total microcystins associates with nitrate and nitrite, and may disrupt the nitrogen cycle, in warm-monomictic lakes of the southcentral United States. *Harmful Algae* **2023**, *130*, 102542.

(4) Organization, W. H. *Guidelines for Drinking-Water Quality*, 4th ed.; World Health Organization, 2011.

(5) Kim, D.; Hong, S.; Choi, H.; Choi, B.; Kim, J.; Khim, J. S.; Park, H.; Shin, K. H. Multimedia distributions, bioaccumulation, and trophic transfer of microcystins in the Geum River Estuary, Korea: Application of compound-specific isotope analysis of amino acids. *Environ. Int.* **2019**, *133* (Pt B), 105194.

(6) Eddy, F. B.; Williams, E. M. Nitrite and Freshwater Fish. *Chem. Ecol.* **1987**, *3* (1), 1−38.

(7) Xiang, L.; Li, Y. W.; Liu, B. L.; Zhao, H. M.; Li, H.; Cai, Q. Y.; Mo, C. H.; Wong, M. H.; Li, Q. X. High ecological and human health risks from microcystins in vegetable fields in southern China. *Environ. Int.* **2019**, *133* (Pt A), 105142.

(8) Chen, J.; Xie, P. Tissue distributions and seasonal dynamics of the hepatotoxic microcystins-LR and -RR in two freshwater shrimps, Palaemon modestus and Macrobrachium nipponensis, from a large shallow, eutrophic lake of the subtropical China. *Toxicon* **2005**, *45* (5), 615−625.

(9) Hosseini, M. J.; Dezhangah, S.; Esmi, F.; S Gharavi-nakhjavani, M.; Hashempour-Baltork, F.; Mirza Alizadeh, A. A worldwide systematic review, meta-analysis and meta-regression of nitrate and nitrite in vegetables and fruits. *Ecotoxicol. Environ. Saf.* **2023**, *257*, 114934.

(10) Zhong, L.; Liu, A. H.; Blekkenhorst, L. C.; Bondonno, N. P.; Sim, M.; Woodman, R. J.; Croft, K. D.; Lewis, J. R.; Hodgson, J. M.; Bondonno, C. P. Development of a Food Composition Database for Assessing Nitrate and Nitrite Intake from Animal-based Foods. *Mol. Nutr. Food Res.* **2022**, *66* (1), No. e2100272.

(11) IARC. *IARC Monographs on the Evaluation of Carcinogenic Risks to Humans Ingested Nitrate and Nitrite, and Cyanobacterial Peptide Toxins*, 2010; Vol. *94*, pp 1−412.

(12) Keita, A. V.; Söderholm, J. D. The intestinal barrier and its regulation by neuroimmune factors. *Neurogastroenterol. Motil.* **2010**, *22* (7), 718−733.

(13) de Vos, W. M.; Tilg, H.; Van Hul, M.; Cani, P. D. Gut microbiome and health: mechanistic insights. *Gut* **2022**, *71* (5), 1020−1032.

(14) Chelakkot, C.; Ghim, J.; Ryu, S. H. Mechanisms regulating intestinal barrier integrity and its pathological implications. *Exp. Mol. Med.* **2018**, *50* (8), 1−9.

(15) Camilleri, M.; Madsen, K.; Spiller, R.; Van Meerveld, B. G.; Verne, G. N. Intestinal barrier function in health and gastrointestinal disease. *Neurogastroenterol. Motil.* **2012**, *24* (6), 503−512.

(16) Chen, Y.; Cui, W.; Li, X.; Yang, H. Interaction Between Commensal Bacteria, Immune Response and the Intestinal Barrier in Inflammatory Bowel Disease. *Front. Immunol.* **2021**, *12*, 761981.

(17) Li, F.; Wang, Z.; Cao, Y.; Pei, B.; Luo, X.; Liu, J.; Ge, P.; Luo, Y.; Ma, S.; Chen, H. Intestinal Mucosal Immune Barrier: A Powerful Firewall Against Severe Acute Pancreatitis-Associated Acute Lung Injury via the Gut-Lung Axis. *J. Inflamm. Res.* **2024**, *17*, 2173−2193.

(18) Wu, J. X.; Huang, H.; Yang, L.; Zhang, X. F.; Zhang, S. S.; Liu, H. H.; Wang, Y. Q.; Yuan, L.; Cheng, X. M.; Zhuang, D. G.; et al. Gastrointestinal toxicity induced by microcystins. *World J. Clin. Cases* **2018**, *6* (10), 344−354.

(19) Kotopoulou, S.; Zampelas, A.; Magriplis, E. Dietary nitrate and nitrite and human health: a narrative review by intake source. *Nutr. Rev.* **2022**, *80* (4), 762−773.

(20) Cosmetic Ingredient Review Expert Panel. Final report of the safety assessment of niacinamide and niacin. *Int. J. Toxicol.* **2005**, *24* (5), 1−31.

(21) Hwang, E. S.; Song, S. B. Possible Adverse Effects of High-Dose Nicotinamide: Mechanisms and Safety Assessment. *Biomolecules* **2020**, *10* (5), 687.
(22) Chen, C.; Yan, W.; Tao, M.; Fu, Y. NAD(+) Metabolism and Immune Regulation: New Approaches to Inflammatory Bowel Disease Therapies. *Antioxidants* **2023**, *12* (6), 1230.
(23) Navarro, M. N.; Gómez de las Heras, M. M.; Mittelbrunn, M. Nicotinamide adenine dinucleotide metabolism in the immune response, autoimmunity and inflammageing. *Br. J. Pharmacol.* **2022**, *179* (9), 1839−1856.
(24) Citi, S. Intestinal barriers protect against disease. *Science* **2018**, *359* (6380), 1097−1098.
(25) An, J.; Liu, Y.; Wang, Y.; Fan, R.; Hu, X.; Zhang, F.; Yang, J.; Chen, J. The Role of Intestinal Mucosal Barrier in Autoimmune Disease: A Potential Target. *Front. Immunol.* **2022**, *13*, 871713.
(26) Lewis, C. V.; Taylor, W. R. Intestinal barrier dysfunction as a therapeutic target for cardiovascular disease. *Am. J. Physiol. Heart Circ. Physiol.* **2020**, *319* (6), H1227−h1233.
(27) Jutfelt, F.; Olsen, R. E.; Björnsson, B. T.; Sundell, K. Parr-smolt transformation and dietary vegetable lipids affect intestinal nutrient uptake, barrier function and plasma cortisol levels in Atlantic salmon. *Aquaculture* **2007**, *273* (2−3), 298−311.
(28) Ito, E.; Kondo, F.; Harada, K. First report on the distribution of orally administered microcystin-LR in mouse tissue using an immunostaining method. *Toxicon* **2000**, *38* (1), 37−48.
(29) Ansari, F. A.; Ali, S. N.; Arif, H.; Khan, A. A.; Mahmood, R. Acute oral dose of sodium nitrite induces redox imbalance, DNA damage, metabolic and histological changes in rat intestine. *PLoS One* **2017**, *12* (4), No. e0175196.
(30) Demircan, M.; Cetin, S.; Uguralp, S.; Karaman, A.; Sezgin, N.; Gozukara, E. M. Plasma D-lactic acid level: a useful marker to distinguish perforated from acute simple appendicitis. *Asian J. Surg.* **2004**, *27* (4), 303−305.
(31) Xiao, L.; Cui, T.; Liu, S.; Chen, B.; Wang, Y.; Yang, T.; Li, T.; Chen, J. Vitamin A supplementation improves the intestinal mucosal barrier and facilitates the expression of tight junction proteins in rats with diarrhea. *Nutrition* **2019**, *57*, 97−108.
(32) Mohammad, S.; Thiemermann, C. Role of Metabolic Endotoxemia in Systemic Inflammation and Potential Interventions. *Front. Immunol.* **2021**, *11*, 594150.
(33) Gonzalez, J. E.; DiGeronimo, R. J.; Arthur, D. E.; King, J. M. Remodeling of the tight junction during recovery from exposure to hydrogen peroxide in kidney epithelial cells. *Free Radical Biol. Med.* **2009**, *47* (11), 1561−1569.
(34) Overgaard, C. E.; Daugherty, B. L.; Mitchell, L. A.; Koval, M. Claudins: control of barrier function and regulation in response to oxidant stress. *Antioxidants Redox Signal.* **2011**, *15* (5), 1179−1193.
(35) Horowitz, A.; Chanez-Paredes, S. D.; Haest, X.; Turner, J. R. Paracellular permeability and tight junction regulation in gut health and disease. *Nat. Rev. Gastroenterol. Hepatol.* **2023**, *20* (7), 417−432.
(36) Auer, I. O. The small intestine as an immune organ. *Fortschr. Med.* **1990**, *108* (15), 292−296.
(37) Thoo, L.; Noti, M.; Krebs, P. Keep calm: the intestinal barrier at the interface of peace and war. *Cell Death Dis.* **2019**, *10* (11), 849.
(38) Li, C.; Ma, D.; Zhou, H.; Zhang, M.; An, L.; Wang, Y.; Wu, C. Effects of different doses lipopolysaccharides on the mucosal barrier in mouse intestine. *Res. Vet. Sci.* **2020**, *133*, 75−84.
(39) Liu, Y.; Yu, X.; Zhao, J.; Zhang, H.; Zhai, Q.; Chen, W. The role of MUC2 mucin in intestinal homeostasis and the impact of dietary components on MUC2 expression. *Int. J. Biol. Macromol.* **2020**, *164*, 884−891.
(40) Gill, N.; Wlodarska, M.; Finlay, B. B. Roadblocks in the gut: barriers to enteric infection. *Cell Microbiol.* **2011**, *13* (5), 660−669.
(41) Van der Sluis, M.; De Koning, B. A.; De Bruijn, A. C.; Velcich, A.; Meijerink, J. P.; Van Goudoever, J. B.; Büller, H. A.; Dekker, J.; Van Seuningen, I.; Renes, I. B.; et al. Muc2-deficient mice spontaneously develop colitis, indicating that MUC2 is critical for colonic protection. *Gastroenterology* **2006**, *131* (1), 117−129.
(42) Ibrahim, A.; Hugerth, L. W.; Hases, L.; Saxena, A.; Seifert, M.; Thomas, Q.; Gustafsson, J.; Engstrand, L.; Williams, C. Colitis-induced colorectal cancer and intestinal epithelial estrogen receptor beta impact gut microbiota diversity. *Int. J. Cancer* **2019**, *144* (12), 3086−3098.
(43) Chen, J. H.; Zeng, L. Y.; Zhao, Y. F.; Tang, H. X.; Lei, H.; Wan, Y. F.; Deng, Y. Q.; Liu, K. X. Causal effects of gut microbiota on sepsis: a two-sample Mendelian randomization study. *Front. Microbiol.* **2023**, *14*, 1167416.
(44) Chen, G.; Kuang, Z.; Li, F.; Li, J. The causal relationship between gut microbiota and leukemia: a two-sample Mendelian randomization study. *Front. Microbiol.* **2023**, *14*, 1293333.
(45) D'Adamo, G. L.; Chonwerawong, M.; Gearing, L. J.; Marcelino, V. R.; Gould, J. A.; Rutten, E. L.; Solari, S. M.; Khoo, P. W. R.; Wilson, T. J.; Thomason, T.; et al. Bacterial clade-specific analysis identifies distinct epithelial responses in inflammatory bowel disease. *Cell Rep. Med.* **2023**, *4* (7), 101124.
(46) Lin, W.; Guo, H.; Wang, L.; Zhang, D.; Wu, X.; Li, L.; Li, D.; Tang, R. Nitrite Enhances MC-LR-Induced Changes on Splenic Oxidation Resistance and Innate Immunity in Male Zebrafish. *Toxins* **2018**, *10* (12), 512.
(47) Lin, W.; Guo, H.; Li, Y.; Wang, L.; Zhang, D.; Hou, J.; Wu, X.; Li, L.; Li, D.; Zhang, X. Single and combined exposure of microcystin-LR and nitrite results in reproductive endocrine disruption via hypothalamic-pituitary-gonadal-liver axis. *Chemosphere* **2018**, *211*, 1137−1146.
(48) Liu, H.; Du, X.; Zhang, Z.; Ge, K.; Chen, X.; Losiewicz, M. D.; Guo, H.; Zhang, H. Co-exposure of microcystin and nitrite enhanced spermatogenic disorders: The role of mtROS-mediated pyroptosis and apoptosis. *Environ. Int.* **2024**, *188*, 108771.
(49) Yang, J.; Zhang, Z.; Du, X.; Wang, Y.; Meng, R.; Ge, K.; Wu, C.; Liang, X.; Zhang, H.; Guo, H. The effect and mechanism of combined exposure of MC-LR and NaNO(2) on liver lipid metabolism. *Environ. Res.* **2024**, *252* (Pt 4), 119113.
(50) Ru, M.; Wang, W.; Zhai, Z.; Wang, R.; Li, Y.; Liang, J.; Kothari, D.; Niu, K.; Wu, X. Nicotinamide mononucleotide supplementation protects the intestinal function in aging mice and D-galactose induced senescent cells. *Food Funct.* **2022**, *13* (14), 7507−7519.
(51) Li, W.; Zhou, Y.; Pang, N.; Hu, Q.; Li, Q.; Sun, Y.; Ding, Y.; Gu, Y.; Xiao, Y.; Gao, M.; et al. NAD Supplement Alleviates Intestinal Barrier Injury Induced by Ethanol Via Protecting Epithelial Mitochondrial Function. *Nutrients* **2022**, *15* (1), 174.
(52) Luciani, A.; Festa, B. P.; Chen, Z.; Devuyst, O. Defective autophagy degradation and abnormal tight junction-associated signaling drive epithelial dysfunction in cystinosis. *Autophagy* **2018**, *14* (7), 1157−1159.
(53) Zhao, Z.; Qu, W.; Wang, K.; Chen, S.; Zhang, L.; Wu, D.; Chen, Z. Bisphenol A inhibits mucin 2 secretion in intestinal goblet cells through mitochondrial dysfunction and oxidative stress. *Biomed. Pharmacother.* **2019**, *111*, 901−908.
(54) Rashid, U.; Khan, M. R.; Sajid, M. Antioxidant, anti-inflammatory and hypoglycemic effects of Fagonia olivieri DC on STZ-nicotinamide induced diabetic rats - In vivo and in vitro study. *J. Ethnopharmacol.* **2019**, *242*, 112038.
(55) Kang, K.; Sun, Y.; Pan, D.; Chang, B.; Sang, L. X. Nicotinamide Ameliorates Dextran Sulfate Sodium-Induced Chronic Colitis in Mice through Its Anti-Inflammatory Properties and Modulates the Gut Microbiota. *J. Immunol. Res.* **2021**, *2021*, 1−19.

https://doi.org/10.1021/acs.jafc.4c06756
J. Agric. Food Chem. XXXX, XXX, XXX−XXX

Supporting Information

Nicotinamide alleviates synergistic impairment of intestinal barrier caused by MC-LR and $NaNO_2$ co-exposure

Xingde Du [a,1], Ruiyang Meng [a,1], Houjiang Wei [b], Zhe Fan [b], Jiankang Wang [b], Shumeng Yuan [a], Kangfeng Ge [a], Haibin Guo [c], Feng Wan [c], Yu Fu [a], Fufang Wang [a], Xinghai Chen [d], Donggang Zhuang [a], Hongxiang Guo [e, *], Huizhen Zhang [a, *]

[a] College of Public Health, Zhengzhou University, Zhengzhou 450001, Henan, China

[b] School of Henan Medical, Zhengzhou University, Zhengzhou 450001, Henan, China

[c] The Reproductive Medicine Center, Henan Provincial People's Hospital, Zhengzhou 450003, Henan, China.

[d] Department of Chemistry and Biochemistry, St Mary's University, San Antonio 78228, Texas, USA.

[e] College of Life Sciences, Henan Agricultural University, Zhengzhou 450002, Henan, China

[1] Xingde Du and Ruiyang Meng contributed equally to this work.

[a, *] First corresponding author: Huizhen Zhang

Phone: +86-15188357252; E-mail: huizhen18@126.com

[e, *] Second corresponding author: Hongxiang Guo

Phone: +86-13643867952; E-mail: guohongxiang06@126.com

1. Materials and Methods

1.1 Regents

Microcystin-LR (purity > 95%) and anti-MC-LR were purchased from Express Technology Co. (Beijing, China). $NaNO_2$ was acquired from Macklin Biochemical Co. (Shanghai, China). Anti-MUC2 (27675-1-AP), anti-ZO-1 (21773-1-AP), anti-Occludin (66378-1-Ig), anti-Claudin-1 (28674-1-AP), anti-β-actin (66009-1-Ig) were purchased from Proteintech Group, Inc (Wuhan, China). Anti-IL-10 (DF6894), anti-IL-4 (AF5142), and anti-IL-1β (DF6251) were purchased from Affinity Biosciences Ltd. Anti-TNF-α (bs-10802R) was purchased from Bioss, and anti-IL-6 (R1412-2) was purchased from HUABIO. Goat Anti-Mouse IgG (CW0102) and Goat Anti-Rabbit IgG (CW0103) were purchased from CoWin Biosciences.

1.2 Animal Treatment

Seven-week-old Specific Pathogen Free (SPF) BALB/c male mice were purchased from Beijing Vital River Laboratory Animal Technology Co., Ltd. (License number: SCXK (Beijing) 2021-0006). After 1 week of adaptive feeding, mice were randomly divided into 9 groups: Control group, M1 group (10 μg/L MC-LR), M2 group (100 μg/L MC-LR), N1 group (30 mg/L $NaNO_2$), N2 group (300 mg/L), M1N1 group (10 μg/L MC-LR+30 mg/L $NaNO_2$), M1N2 group (10 μg/L MC-LR+300 mg/L $NaNO_2$), M2N1 group (100 μg/L MC-LR+30 mg/L $NaNO_2$), M2N2 group (100 μg/L MC-LR+300 mg/L $NaNO_2$), 10 mice in each group, the exposure duration was 6 months. At the end of the exposure experiment, the mice were executed under anesthesia, and the jejunal tissues

were taken for subsequent experimental studies. The jejunum, with its complex structure and abundant villi, is crucial for nutrient absorption. It also provides a key habitat for intestinal microbes and plays significant immune roles, making it an ideal model for studying intestinal barrier functions [1, 2]. All animal protocols were reviewed and approved by the Animal Ethics Committee of Zhengzhou University (ethical approval number: ZZUIRB2022-09).

Considering the species variation, the TDIs of MC-LR and $NaNO_2$ were multiplied by an uncertainty factor of 10, that is, 10 μg/L MC-LR and 30 mg/L $NaNO_2$ were used for the mouse exposure experiments, which approximates the daily exposure levels in humans [3]. Referring to the study by Guo et al.[4], The concentration of 100 μg/L MC-LR and 300 mg/L $NaNO_2$ were used to simulate the condition of the high-exposure risk population in this study. This experimental design allowed our results to reflect the impact of MC-LR and $NaNO_2$ co-exposure on human health to a certain extent.

1.3 Cell Experiments

Human colorectal adenocarcinoma cells (Caco-2 cells) purchased from Pricella Life Science & Technology Co., Ltd. were cultured in Minimum Essential Medium (MEM) with 20% Fetal Bovine Serum (BioChannel Biological Technology Co., Ltd.) at 37°C in a humidified CO_2 incubator. After digestion of the Caco-2 cells, the cells were transferred into a 96-well cell culture plate (NEST Biotechnology) with approximately 3000 cells per well. The 24-hour half maximal inhibitory concentration (IC_{50}) of MC-LR and $NaNO_2$ on Caco-2 cells, as well as the 24-hour no-observed-

adverse-effect-level (NOAEL) of Nicotinamide (NAM, MedChemExpress, USA), were determined using Cell Counting Kit-8 (M4839, AbMole, USA) and a microplate reader at 450 nm. In this study, Caco-2 cells were exposed to 1/2 IC_{50} of MC-LR (18 μM) and $NaNO_2$ (29 μM) for 24 h. NAM was applied at its NOAEL of 1 mM for intervention treatment.

1.4 Hematoxylin and Eosin (H&E) Staining

The extracted jejunal tissues of mice were fixed in 4% paraformaldehyde at 4°C for 24 hours. The tissues were then embedded in paraffin and cut into approximately 4 μm thick sections. Sections were deparaffinized in xylene for 10 minutes, followed by a series of graded alcohols (100%, 95%, and 70%) for rehydration. Next, sections were stained with hematoxylin for 5 min and eosin for 1 min, then dehydrated, cleared in xylene, and mounted. Morphological changes were observed under a microscope (Nikon Eclipse E100, Japan). Three different mice were tested in each group.

1.5 Assay of $NaNO_2$ Concentration in Intestinal Tissues

The jejunal tissues were weighed about 0.5 g, and the tissues were ground and ultrasonically broken. The concentration of $NaNO_2$ in the samples was determined using the Nitrite Content Detection Kit (Solarbio, China). According to the instructions of the kit, the extract reagents were added sequentially and centrifuged at 10000 rpm/min for 15 min. The supernatant was measured at 540 nm on a Multi-mode Microplate Reader. Three samples per group were used for the experiment.

1.6 Western Blot and Dot Blot

Total proteins from jejunal tissues and Caco-2 cells were extracted by RIPA lysis buffer containing a 1% protease inhibitor. The protein concentration was measured using the BCA Protein Assay Kit (Beyotime, Shanghai, China) following the manufacturer's protocol. Proteins were size-fractionated by 10% SDS-PAGE and transferred to polyvinylidene fluoride (PVDF) membranes. After blocking for 2 hours with TBST containing 5% skim milk, the membranes were incubated overnight at 4°C with primary antibodies. Following five washes with TBST, HRP-coupled secondary antibodies were incubated with the membranes for 2 h at room temperature. Finally, the membranes were washed five times. The protein bands were visualized using the enhanced chemiluminescence detection kit. All samples were performed in triplicate. The ImageJ software was used to analyze the intensity of the bands.

As for the Dot Blot, Caco-2 cell proteins were extracted using the Total protein extraction kit (Beijing Solarbio Science & Technology Co., Ltd.), and the protein concentration was determined and standardized. Next, 5 μg of the protein sample was spotted onto the NC membrane and allowed to dry at room temperature. The membrane was blocked with 5% skim milk, washed five times with TBST, and incubated overnight with the primary antibody (anti-MUC2). The following day, the membrane was washed five times with TBST, incubated with the secondary antibody for 2 h, washed again, and visualized using a chemiluminescence imaging system.

1.7 Determination of Serum D-Lactic Acid, Diamine Oxidase, and Lipopolysaccharide Binding Protein (LBP)

Fresh blood was collected from mice, placed at room temperature for 1 h, centrifuged at 3000 rpm for 10 min, and the serum was collected.

The D-lactic Acid Assay Kit (Elabscience® Biotechnology Co., Ltd) was used to determine the contents of D-lactic acid. First, 5 μL of standards at different concentrations or the samples were added to the wells of the ELISA plate. Next, 100 μL of enzyme working solution was added to each well, followed by 20 μL of chromogenic agent, which was incubated at 37°C for 10 min. Then, 180 μL of stop solution was added to each well. Finally, the Optical Density (OD) value of each well at 530 nm was measured using a multi-mode microplate reader. The concentration of D-lactic acid was calculated according to the standard curve.

The Diamine oxidase Assay kit (NJJCBIO, China) was used to determine the contents of Diamine oxidase. First, the UV spectrophotometer was set to 340 nm and zeroed with distilled water in a quartz cuvette. Then, an 80 μL sample was mixed with 800 μL working solution in a test tube and transferred to the cuvette, where absorbance A1 was measured after 20 s. Then, the solution was returned to the test tube and incubated at 37°C for 10 min, after which absorbance A2 was measured 20 s later. The activity of diamine oxidase was analyzed using the formula from the kit's instructions.

The Lipopolysaccharide Binding Protein ELISA Kit (ABclonal Technology, Wuhan, China) was used to determine the contents of LBP. First, 100 μL of standards

or samples were added to each well and incubated for 2 h at 37°C, followed by three washes. Next, 100 μL of working biotin-conjugate antibody was added and incubated for 1 h at 37°C, then washed three times. Following this, 100 μL of working streptavidin-HRP was added and incubated for another hour at 37°C, followed by three washes. Then, 100 μL of substrate solution was added and incubated for 15min at 37°C in the dark. Finally, 50 μL of stop solution was added, and the optical density was measured within 5 min at 450 nm. The content of LBP was calculated according to the standard curve.

Three mice per group were detected for the experiment.

1.8 Determination of NAM

NAM levels in mouse jejunal tissues and Caco-2 cells were measured using Human and Mouse Nicotinamide ELISA kits (Jiangsu Meimian Industrial Co., Ltd). Briefly, the NAM standard was diluted in a gradient. Fifty microliters of both diluted standard and test samples were added to each well of the enzyme-containing 96-well plate. The plate was incubated at 37°C for 30 min, then washed for 5 times. Following this, 50 μL of enzyme-labeled reagent was added to each well, and the plate was incubated at 37°C for 10 minutes before being washed five times. Finally, 50 μL of Stop Solution was added, and the OD value at 450 nm was measured using a multi-mode microplate reader. NAM levels were calculated according to the standard curve.

1.9 Transmission Electron Microscope

Mouse jejunal tissues were cut into 1 mm^3 and fixed in 2.5% glutaraldehyde,

avoiding light for 24 h. After washing with PBS to remove excess fixative, the samples were post-fixed with 1% osmium tetroxide for 2 h. Subsequently, dehydration was performed through a graded series of ethanol solutions, followed by embedding in epoxy resin and polymerization at 60°C. Ultra-thin sections of 60-80 nm were obtained using an ultra-microtome. The sections were stained with uranyl acetate and lead citrate solutions to improve contrast and then dried. Images were captured and scanned using a transmission electron microscope (Hitachi HT7800, Japan).

1.10 Real-Time Quantitative PCR (qPCR)

Total RNA was extracted using the TRIZOL reagent (TaKaRa, Dalian, China). The concentration, RNA purity, and DNA contamination were analyzed using a NanoDrop 2000 spectrophotometer (Thermo, USA). RNA pellet was collected and dissolved in DNase/RNase-free water for RNA integrity analysis using the Agilent 2100 Bioanalyzer (Agilent Technologies, USA). Then, the extracted RNA (1 μg) was reverse-transcribed using an EasyScript First-Strand cDNA synthesis super mix kit (Thermo Fisher SCIENTIFIC, K1622) (42°C for 60 min and 70°C for 5min). qPCR was performed using QuantStudio 7 Flex real-time PCR system (Thermo Fisher SCIENTIFIC, USA) and SYBR premix Ex Taq (TaKaRa, Dalian, China). The PCR reaction was performed at 95 °C (5 min), followed by 40 cycles of denaturation for 95 °C (15 s), 60 °C (20 s), and 72 °C (20 s). The relative quantification values for mRNA were calculated by the $2^{-\Delta\Delta Ct}$ method using the *β-actin* gene as an internal reference. Primer sequences used in the qPCR experiment are shown in Table 1. Three

mice per group were tested for the experiment.

Table S1 Primer sequences used in qPCR

Genes	Forward primers (5′-3′)	Reverse primers (5′-3′)
Tjp1	*CGAGGCATCATCCCAAATAAGA*	*TCCAGAAGTCTGCCCGATCAC*
Ocln	*TGAAAGTCCACCTCCTTACAGA*	*CCGGATAAAAAGAGTACGCTGG*
Cldn1	*TGCCCCAGTGGAAGATTTACT*	*CTTTGCGAAACGCAGGACAT*
Cldn2	*CAACTGGTGGGCTACATCCTA*	*CCCTTGGAAAAGCCAACCG*
Cldn3	*ACCAACTGCGTACAAGACGAG*	*CAGAGCCGCCAACAGGAAA*
Cldn7	*GGCCTGATAGCGAGCACTG*	*GTGACGCACTCCATCCAGA*
Tnfa	*GAGGCCAAGCCCTGGTATG*	*CGGGCCGATTGATCTCAGC*
Il10	*GCTCTTACTGACTGGCATGAG*	*CGCAGCTCTAGGAGCATGTG*
Il4	*GGTCTCAACCCCCAGCTAGT*	*GCCGATGATCTCTCTCAAGTGA*
Il1b	*GAAATGCCACCTTTTGACAGTG*	*TGGATGCTCTCATCAGGACAG*
Il6	*ACTCACCTCTTCAGAACGAATTG*	*CCATCTTTGGAAGGTTCAGGTT*
Ifng	*TAACTCAAGTGGCATAGATGTGG*	*GACGCTTATGTTGTTGCTGATG*
Muc2	*AGGGCTCGGAACTCCAGAAA*	*CCAGGGAATCGGTAGACATCG*
β-actin	*GTGCTATGTTGCTCTAGACTTCG*	*ATGCCACAGGATTCCATACC*

1.11 Periodic Acid-Schiff Staining (PAS Staining)

Paraffin sections were deparaffinized by incubating in xylene and then rehydrated through a series of graded alcohols. Next, sections were immersed in pure water and then treated with 1% aqueous periodate for 30 min. Schiff's reagent was applied to stain the sectioned tissue for 20 min. After staining, the sections were counterstained with hematoxylin for 5 minutes to visualize cell nuclei. Following routine dehydration, the sections were cleared and sealed. Images were collected and analyzed after observation under a microscope. Three samples per group were tested for the experiment.

1.12 Immunohistochemical Staining

Paraffin sections were deparaffinized in xylene and rehydrated through a series of graded alcohols to water, followed by antigen retrieval using a citrate buffer or a specific retrieval solution. Sections were incubated with 3% hydrogen peroxide for 25 min at room temperature, avoiding light. Following this, the sections were blocked with bovine serum albumin for 30 min. Then, the sections were incubated overnight at 4°C with primary antibody anti-MUC2 (1:2000). After washing with PBS, the sections were incubated with an HRP-conjugated secondary antibody at room temperature for 50 min. Followed by 3,3'-Diaminobenzidine and hematoxylin were applied for staining. The sections were washed in pure water and then dehydrated, cleared, and sealed. The images were captured under a microscope and relatively quantitatively analyzed by ImageJ. Three mice per group were tested for the experiment.

1.13 16s RNA Sequencing

Fresh feces of 5 mice in the control group, M2 group, N2 group, and M2N2 group were collected, respectively. Bacterial DNA from mouse feces was isolated, and the integrity and concentration of DNA were examined by NanoDrop 2000 spectrophotometer (Thermo Fisher Scientific, USA) and agarose gel electrophoresis, respectively. PCR amplification of the V3-V4 hypervariable regions of the bacterial 16S rRNA gene was carried out in a 25 μL reaction using universal primer pairs (343F: 5’-TACGGRAGGCAGCAG-3’; 798R: 5’-AGGGTATCTAATCCT-3’). The sequencing was performed using the Illumina NovaSeq6000 sequencing system. The

raw sequencing data were quality controlled by low-quality sequences filtering, denoised, merged, and detected and cut off the chimera reads. The obtained representative sequences were annotated and blasted against the Silva (version 138) database using a q2-feature-classifier with the default parameters. The 16S rRNA gene amplicon sequencing and analysis were conducted by OE Biotech Co., Ltd. (Shanghai, China).

1.14 Statistical Analysis

Data were statistically analyzed using SPSS 21.0, and experimental data were presented as mean ± standard deviation ($\overline{x} \pm SD$). A one-way analysis of variance (one-way ANOVA) was used for comparisons between groups. Multiple comparisons were performed using the student-Newman-Keuls (SNK) test if the variance was homogeneous, or the Dunnett T3 test if the variance was inhomogeneous. A statistically significant difference was indicated at $P < 0.05$. Two-way ANOVA analyzed the interaction effects of MC-LR and $NaNO_2$. A significant interaction was present when $P_{interaction} < 0.05$. Next, the Additive index was used to identify the type of interaction

Reference

(1) Dou, X.; Ma, Z.; Yan, D.; Gao, N.; Li, Z.; Li, Y.; Feng, X.; Meng, L.; Shan, A. Sodium butyrate alleviates intestinal injury and microbial flora disturbance induced by lipopolysaccharides in rats. *Food & function* **2022**, *13* (3), 1360-1369.

(2) Jiang, Q.; Tian, J.; Liu, G.; Yin, Y.; Yao, K. Endoplasmic Reticulum Stress and Unfolded Protein Response Pathways Involved in the Health-Promoting Effects of Allicin on the Jejunum. *J Agric Food Chem* **2019**, *67* (21), 6019-6031.

(3) Nair, A.; Morsy, M. A.; Jacob, S. Dose translation between laboratory animals and human in preclinical and clinical phases of drug development. *Drug development research* **2018**, *79* (8), 373-382.

(4) Guo, Y.; Du, X.; Wang, F.; Fu, Y.; Guo, X.; Meng, R.; Ge, K.; Zhang, S. Co-exposure of microcystin-LR and nitrite induced kidney injury through TLR4/NLRP3/GSDMD-mediated pyroptosis. *Ecotoxicology and environmental safety* **2024**, *281*, 116629.